Scripta Materialia 127 (2017) 173–177

Contents lists available at ScienceDirect

Scripta Materialia

journal homepage: www.elsevier.com/locate/scriptamat

Regular article

Fracture behavior of an austenitic stainless steel with nanoscale deformation twins

L. Xiong [a], Z.S. You [a,b], L. Lu [a,*,1]

[a] Shenyang National Laboratory for Materials Science, Institute of Metal Research, Chinese Academy of Sciences, 72 Wenhua Road, Shenyang 110016, People's Republic of China
[b] Herbert Gleiter Institute of Nanoscience, Nanjing University of Science and Technology, 200 Xiaolingwei Street, Nanjing 210094, People's Republic of China

ARTICLE INFO

Article history:
Received 29 June 2016
Received in revised form 6 September 2016
Accepted 10 September 2016
Available online xxxx

Keywords:
Nanotwinned stainless steel
Fracture toughness
Shear deformation
Void nucleation

ABSTRACT

A bulk nanotwinned austenitic stainless steel containing a large volume fraction of deformation twins was produced by dynamic plastic deformation. The tensile tests and *J*-integral fracture toughness measurements indicate that this steel exhibits a combination of high strength ($\sigma_{ys} = 920$ MPa) and considerable fracture toughness ($K_{JC} > 126$ MPa m$^{1/2}$). The fracture is associated with localized shear band induced destruction of the nanotwinned structure and with micro-void development at the generated nanoscale large angle grain boundaries within the shear bands, which consumes large plastic energy and contributes the fracture resistance.

Materials with embedded nanoscale twins have attracted extensive interest in recent years due to their novel mechanical properties, such as an unusual combination of high strength and good tensile ductility, enhanced strain hardening capacity, and improved fatigue resistance [1–6]. These properties have an important bearing on the special characteristics of twin boundaries (TBs) that not only restrict dislocation propagation, but also react with and accumulate dislocations [3,5]. Nanotwinned materials hold promise for applications as structural components, in which a fracture mechanics evaluation on their fracture resistance is highly demanded to ensure structural reliability and safety. However, in contrary to the strengthening and deformation mechanisms that have been extensively studied [7–10], investigations regarding the fracture mechanism of nanotwinned metals are extremely scarce.

The fatigue crack growth tests by Singh et al. [6] revealed that ultrafine-grained Cu with nanoscale twins exhibits enhanced damage tolerance in comparison to twin-free samples. Through in-situ transmission electron microscope (TEM) investigations, Shan et al. [11] observed that crack grew in a zig-zag path across nano-twin lamellae. The molecular dynamic (MD) simulations by Zeng et al. [12] and by Kim et al. [13] further demonstrated that nanoscale twins not only substantially blunted micro-crack tips, but also served as crack bridging ligaments as the crack advanced. These experimental investigations and MD simulations indicate that the incorporation of high-density nanoscale twins is potentially beneficial to provide enhanced damage tolerance [2,6,12–15].

However, the studies carried out so far majorly focus on the fracture process of nanotwinned thin sheets that are inevitably in plane stress state, which may be distinctly different from the fracture behavior of bulk samples in plane strain state. Accurate evaluation of the intrinsic plain strain fracture toughness of nanotwinned materials, which enables the damage tolerant design required for many structural applications, is still lacking. The scarcity of such researches can be in part ascribed to the fact that current preparation techniques, such as electrodeposition and magnetron sputtering [4,16,17], do not deliver adequate sample volumes for fracture toughness tests.

Contrarily to growth nano-twins, nanoscale deformation twins are more easily generated during plastic deformation of metals with medium or low stacking fault energies, which makes it feasible to prepare bulk nanotwinned metals [18–20]. For instance, dynamic plastic deformation (DPD) has been demonstrated to be a practical approach to introduce nanotwinned structures in various kinds of bulk metals and alloys [21–24]. In the present study, a large volume fraction (~60%) of nanoscale deformation twins is introduced into a 316L stainless steel (SS) by DPD under a controlled compression strain. The fracture toughness of this bulk nanotwinned steel is then evaluated by elastic-plastic *J*-integral method, and the fracture process is discussed based on microstructural characterization and fractographic analysis.

The material used is a commercial AISI 316L SS with a composition of Fe-16.42Cr-0.02C-0.37Si-1.42Mn-0.011S-0.040P (wt.%). The as-received steel was first annealed at 1200 °C for 1 h to generate uniform equiaxed austenitic grains with an average size of ~100 μm, and then treated by the DPD technique at ambient temperature. The setup and

* Corresponding author.
E-mail address: llu@imr.ac.cn (L. Lu).
[1] This author was an Editor of the journal during the review period of the article. To avoid a conflict of interest, Irene J. Beyerlein acted as Editor for this manuscript.

http://dx.doi.org/10.1016/j.scriptamat.2016.09.012
1359-6462/

processing parameters of the DPD treatment were described in detail elsewhere [25]. Cylindrical samples with a diameter of 23 mm and a height of 4.5 mm were compressed into disks with final dimensions of 28 mm in diameter and 3 mm in height. Accordingly, the imposed total true strain, defined as $\varepsilon = \ln(h_i/h_f)$, is about 0.4, where h_i and h_f are the initial and final height of the treated sample, respectively. This strain was selected in purpose to make the volume fraction of deformation twins as large as possible.

The fracture toughness was assessed by *J*-integral measurement using a single specimen procedure according to ASTM E1820-11 [26]. For the *J*-integral test, miniaturized single edge-notched bend (SEB) specimen with a thickness of 2 mm, a width of 4 mm, a span distance of 16 mm and a total length of 22 mm, was machined from the DPD disk, with the thickness direction of the SEB specimen corresponding to that of the DPD disk. The crack plane normal direction and the crack propagation direction are parallel to the tangential and radial directions of the DPD disk, respectively. The SEB specimens were first notched by electro-discharge machine and then fatigue pre-cracked to a total original crack length a_0 of ~2 mm. Finally, the samples were monotonically bent to extend the sharp crack on an Instron 5848 micro-tester at a constant displacement rate of ~0.3 mm min^{-1}. The corrected cross-head displacement of the tensile machine was used to represent the load-line displacement *v* [27], and the instantaneous crack length *a* was monitored using direct current potential drop method [28]. With the synchronously recorded *P*, *v*, and *a*, the *J*-integral resistance curve was computed following the standardized procedure [26].

To reveal the fracture process, the microstructure of the as-treated and fracture tested DPD sample was characterized by a scanning electron microscope (SEM; FEI NovaNano 430) and a transmission electron microscope (TEM; JEOL 2010). The fracture surface was examined by the SEM, and by a confocal laser scanning microscope (CLSM; Olympus LEXT OLS4000) to determine the three-dimensional topography.

Cross-sectional SEM observations of the DPD sample (Fig. 1a) indicate that the grain boundaries (GBs) are still distinguishable and the original equiaxed grains become slightly elongated normal to the compression direction. The transverse grain size ranges from 20 μm to 100 μm, with an average value of 50 μm. Numerous deformation bands making angles close to ±45° with respect to the DPD compression direction can be detected in most grains. Closer TEM observations (Fig. 1b) reveal that these bands are deformation twins, verified by the corresponding selected area electron diffraction (SAED) pattern. Most of the twin/matrix lamellae are thinner than 200 nm and the average thickness is ~40 nm. Inside the twin/matrix lamellae, there are numerous dislocations accumulating at the TBs. Statistical analysis indicates that >60% of the deformed grains possess such deformation twins. No shear bands or cracks were detected due to the small imposed strain. Besides the grains with deformation twins, there are also some deformed grains with only dislocation tangles and/or dislocation cells, see Fig. 1c and the single crystal SAED pattern, corresponding to the featureless areas in Fig. 1a. These twin-free grains were found to disperse among the nanotwinned grains and to occupy the remaining 40% volume.

Tensile tests show that the as-annealed coarse-grained 316L SS possesses a yield strength σ_{ys} of 275 ± 5 MPa and an ultimate tensile strength σ_{uts} of 585 ± 9 MPa. After the DPD treatment, σ_{ys} is increased to 920 ± 20 MPa and σ_{uts} to 962 ± 20 MPa. Both σ_{ys} and σ_{uts} are remarkably improved as compared to those of the coarse-grained counterpart, which has been demonstrated to arise out of the nanoscale deformation twins impeding dislocation movement [22,23]. In contrary, the DPD treatment results in obvious reduction in tensile ductility. The uniform elongation ε_u decreases from 58 ± 5% at the coarse-grained state to only about 1 ± 0.5%, and the elongation to failure ε_f is reduced from 67 ± 4% to 15 ± 1%.

Fig. 2a shows the representative curves of the force *P* and the instantaneous electric resistance *R* as a function of load-line displacement *v* for the DPD sample. *R* values were used to calculate the crack extension Δ*a* during bending by using a calibrated *R*–*a* curve. The calculated *J*–Δ*a* curves (Fig. 2b) indicate that the DPD sample exhibits stable crack growth and the crack propagation resistance significantly increases as the crack extends, analogous to the fracture tests of other nanostructured metals [29–31]. The crack blunting line is represented by $J = 2\sigma_Y \Delta a$, where the effective yield strength $\sigma_Y = 941$ MPa is the average

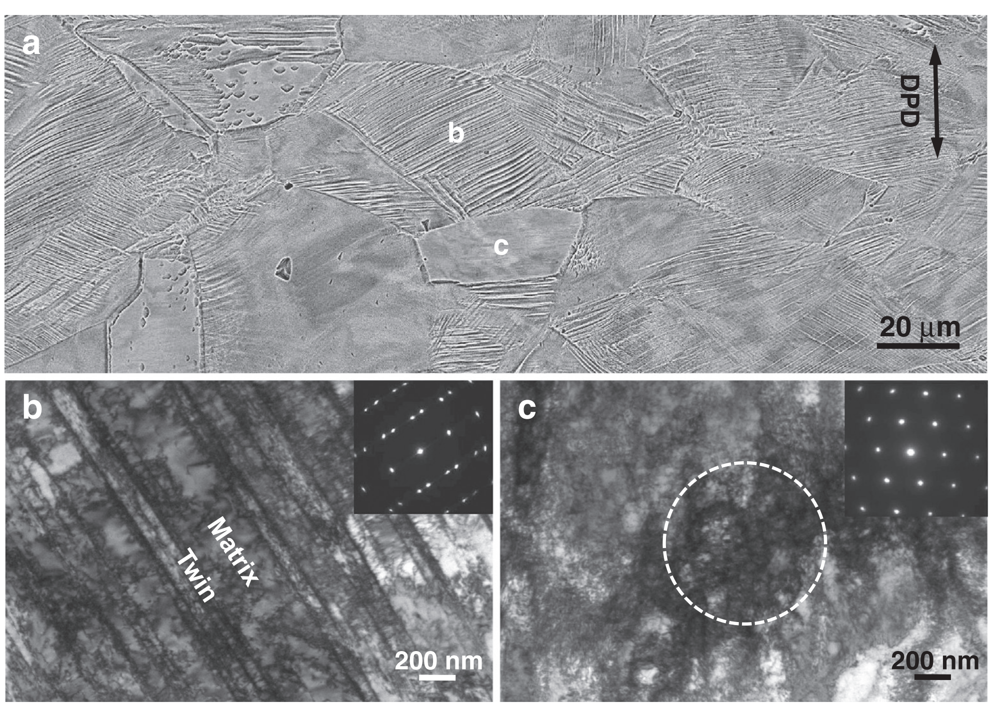

Fig. 1. (a) SEM observations of the cross-sectional microstructure of the DPD sample, showing numerous deformation bands inside most of the original coarse grains. (b) and (c) TEM images of the deformation twins and the deformed coarse grains, corresponding to b and c regimes in (a), respectively.